# One-pot synthesis of AuPt alloyed nanoparticles by intense x-ray irradiation

**11 authors**, including:

Sheng-Feng Lai
Academia Sinica
**29** PUBLICATIONS **296** CITATIONS

SEE PROFILE

Hsianghsin Chen
Academia Sinica
**51** PUBLICATIONS **632** CITATIONS

SEE PROFILE

Wen-Chang Chen
National Taiwan University
**365** PUBLICATIONS **11,190** CITATIONS

SEE PROFILE

Yi Yun Chen
Academia Sinica
**9** PUBLICATIONS **161** CITATIONS

SEE PROFILE

**Some of the authors of this publication are also working on these related projects:**

Antibiofouling coatings View project

Electrospun Nanofibers on the optoelectronics View project

# One-pot synthesis of AuPt alloyed nanoparticles by intense x-ray irradiation

**Cheng-Liang Wang**[1,6]**, Bo-Jun Hsao**[1]**, Sheng-Feng Lai**[1,2]**,
Wen-Chang Chen**[2]**, Hsiang-Hsin Chen**[1]**, Yi-Yun Chen**[1]**,
Chia-Chi Chien**[1,3]**, Xiaoqing Cai**[1]**, Ivan M Kempson**[1]**, Y Hwu**[1,3,4,6]
**and G Margaritondo**[5]

[1] Institute of Physics, Academia Sinica, Nankang, Taipei 11529, Taiwan

[2] Department of Chemical and Materials Engineering, National Yulin University of Science
and Technology, Douliou, Yunlin 64002, Taiwan

[3] Department of Engineering and System Science, National Tsing Hua University,
Hsinchu 30013, Taiwan

[4] Institute of Optoelectronic Sciences, National Taiwan Ocean University, Keelung 20224,
Taiwan

[5] Ecole Polytechnique Fédérale de Lausanne (EPFL), CH-1015 Lausanne, Switzerland

E-mail: clwang@phys.sinica.edu.tw and phhwu@.sinica.edu.tw

**Abstract**
We synthesized AuPt alloyed nanoparticles in colloidal solution by a one-pot procedure based
on synchrotron x-ray irradiation in the presence of PEG (polyethylene glycol). The exclusive
presence of alloyed nanoparticles with fcc structure was confirmed by several different
experiments including UV–vis spectroscopy, x-ray diffraction (XRD) and transmission electron
microscopy (TEM). The composition of the AuPt alloyed nanoparticles can be varied in a
continuous fashion by simply varying the feed ratios of Au and Pt precursors. The nanoparticles
exhibited colloidal stability and biocompatibility, important for potential applications.

S Online supplementary data available from stacks.iop.org/Nano/22/065605/mmedia

(Some figures in this article are in colour only in the electronic version)

## 1. Introduction

Bimetallic nanoparticles (NPs) are potentially interesting for applications such as catalysis, electronics and optical devices [1–4]. This is particularly true for Au/Pt NPs even if bulk Au and Pt are immiscible at low temperature [5, 6], since they combine the catalytic effects of each metal and open possible synergies [7–10] related, for example, to the d-band shift [11]. Such NPs could be specifically exploited in electrocatalysis, selective oxidation and dehydrogenation catalysts [12–14].

Theory predicted [15, 16] AuPt NP alloying but the practical fabrication requires complicated processes [17]. The different reduction kinetics and potentials for Au and Pt ions [18] favor the formation of core–shell or gradient alloy NPs [19, 15, 20–22]. The use of post-synthesis annealing [23–25] to solve these problems can lead to uncontrollable nanostructures. Several different strategies were thus proposed and realized [26–28] to avoid it. All of them relied on the facilitation of fast reduction and a timely growth termination by surfactant molecules.

Here we demonstrate an alternate approach along this line: the production of high quality AuPt alloyed NPs by intense ($>10^{14}$ photon mm$^{-2}$ s$^{-1}$) x-ray irradiation from a synchrotron in the presence of polyethylene glycol (PEG)—a common biocompatible molecule known to prevent NP aggregation. The reduction was caused by radiolysis products such as electrons and/or other free radicals [29–32] and no additional reducing agents were added in the solution. The high x-ray penetration guarantees a uniform Au and Pt ion reduction over the entire solution volume—difficult to obtain with other methods.

We recently demonstrated NP growth by synchrotron x-ray irradiation for several monometallic systems including

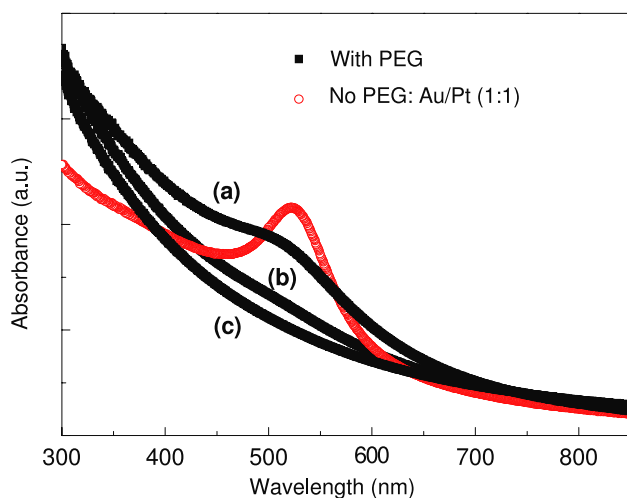[6] Authors to whom any correspondence should be addressed.

**Figure 1.** UV–vis absorption spectra of NPs synthesized by synchrotron x-ray irradiation in the absence (open circles) and in the presence of PEG: Au/Pt = 4:1 (a), 1:1 (b) and 1:4 (c).

Au [33], Ag [19], NiP [34], and others, producing well-dispersed, stable colloids. The exposure time in each case was less than a second, compared with the several hours required with $\gamma$-rays [35] or x-rays [36] from conventional sources.

In the present study, we tackled the first application to alloyed NPs. The fast irradiation appears quite important for bimetallic NPs: slow $\gamma$-ray irradiation resulted, for example, in Ag/Pt NPs with core–shell-like structure [35]. With fast reduction by irradiation we could instead obtain excellent results as confirmed by XRD, TEM UV–vis spectroscopy and Fourier transform infrared spectroscopy (FTIR).

## 2. Experimental details

HAuCl$_4$·3H$_2$O (Aldrich, MO, US) and H$_2$PtCl$_6$·6H$_2$O (Aldrich, MO, US) were used for the precursor solution together with PEG (MW 6000, Showa Inc., Japan). The Au$^{3+}$/Pt$^{4+}$ molar ratios ranged from 1/4 to 4/1 and the total solution concentration was fixed at 1 mM. The solution (with or without the addition of PEG (0.5 ml, 2 wt%)) was put in a polypropylene conical tube and exposed to the x-rays at the BL01A beam line of the NSRRC (National Synchrotron Radiation Research Center) storage rings. The detailed parameters of the irradiation light source were reported elsewhere [33].

The irradiation-induced formation of alloyed NPs in the presence of PEG was verified with different methods. First, visual inspection showed that the rapid changes in color during irradiation from the original light yellow of the solution are quite different with and without PEG: in the absence of PEG, the irradiated colloids all become red, independent of the solution composition, while with PEG, the color changes to brownish within a few seconds. This last result also indicates that the reduction reaction occurs during the irradiation on the scale of seconds.

The nanoparticles were analyzed by x-ray diffraction (XRD) and transmission electron microscopy (TEM) to
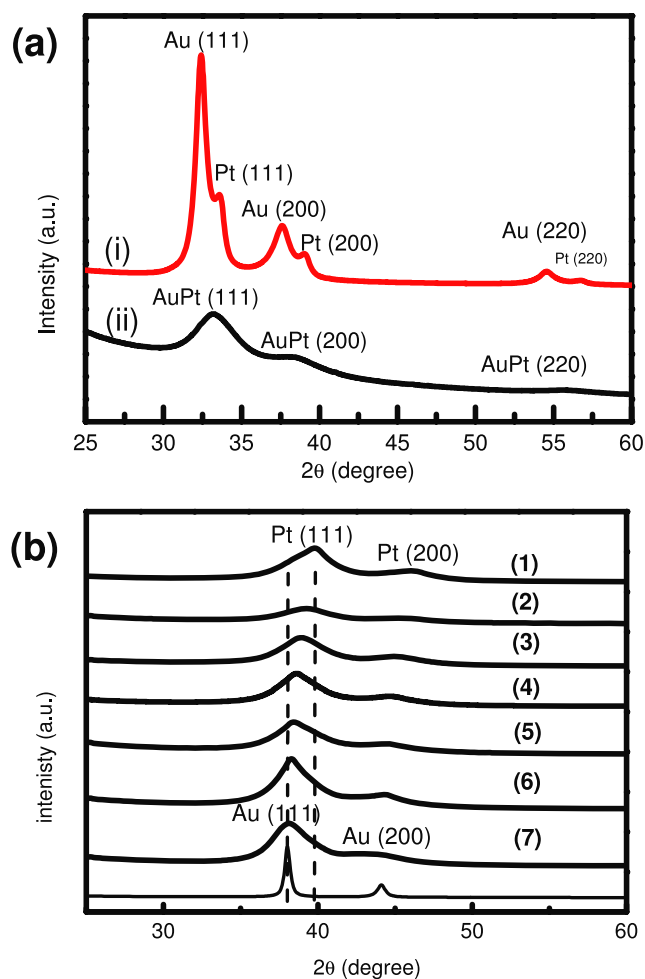




**Figure 2.** (a) $\theta$–$2\theta$ XRD patterns of NPs synthesized from a solution with 1:1 Au/Pt ratio without PEG (i) and with PEG (ii) and (b) $\theta$–$2\theta$ XRD patterns of NPs synthesized from a solution with different molar ratios of Au/Pt ions.

determine their size, composition and crystalline structures. XRD measurements were performed using x-rays from the wiggler beamline BL17A (wavelength = 0.1333 nm) at National Synchrotron Radiation Research Center (NSRRC, Hsinchu, Taiwan). The results were interpreted using JCPDS indexing with correction for the different x-ray source. High-resolution TEM and the selected area electron diffraction measurements were performed on dried nanoparticles on carbon-coated Cu grids using a field emission gun TEM operating at 200 kV (JEOL JEM-2100 F) which is also equipped with an energy dispersive x-ray analyzer (EDX, Link ISIS 300). UV–vis absorption spectra were recorded using a GBC UV/VIS 916 spectrophotometer.

## 3. Results and discussion

UV–vis spectroscopy confirmed the differences between irradiation with or without PEG. Figure 1 shows the results for different Au/Pt concentration ratios in the precursor solutions. The ~520 nm absorption peak due to the surface plasmon resonance (SPR) of monometallic Au NPs is clearly seen
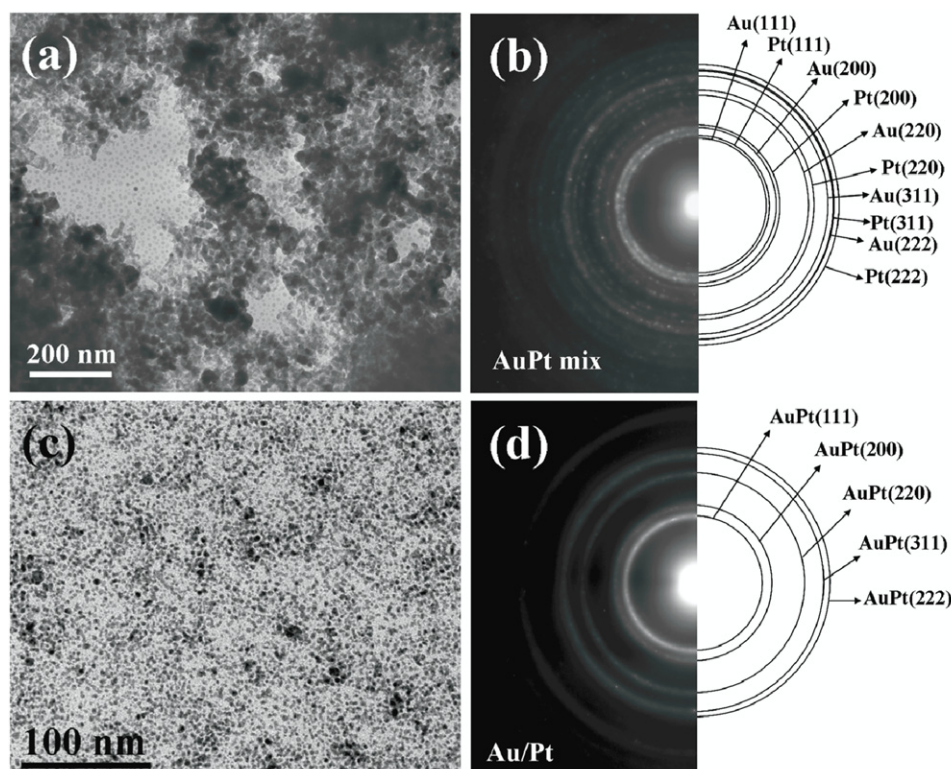
**Figure 3.** TEM images and SAED patterns of NPs synthesized from a solution with 1:1 Au/Pt ratio without PEG (a), (b) or with PEG (c), (d).

without PEG but is suppressed by the presence of PEG. This indicates that PEG prevents the formation of monometallic Au NPs. We can estimate that the Au NP concentration with PEG is less than 0.05 mM. With 4:1 (Au/Pt) concentration, the characteristic 520 nm Au SPR peak appears stronger and narrower than that of 1:1, indicating the stronger presence of Au in the AuPt nanoparticles. We also found that for a ratio of 4 of Au/Pt, 80% of the sites are occupied by Au atoms and the quenched absorption peak is believed to be from SPR of Au.

Figure 2(a) shows $\theta$–$2\theta$ XRD scans of NPs from a solution with 1:1 Au/Pt ratio with and without PEG addition. The diffraction peaks without PEG correspond to the Au(111), Pt(111), Au(200), Pt(200), and Pt(220) crystal planes. With PEG, the broad peaks indicate a AuPt alloy with fcc structure and therefore bimetallic NPs with no monometallic NPs. The diffraction peak widths yield an average particle size ∼2.85 nm. By varying the feed ratios of Au and Pt ions, the composition of Au and Pt in the resulting NPs can be proportionally adjusted. X-ray diffraction tests, as in figure 2(b), show that the diffracted peaks of the resulting AuPt NPs are between those of pure Au and pure Pt NPs which implies that the single-phase alloyed structure of fcc is successfully synthesized.

The NP composition was further analyzed by nano-EDX (energy dispersive x-ray) spectroscopy again for a solution with 1:1 Au/Pt ratio in the presence of PEG. The results indicated a AuPt composition of ∼53–47 consistent with the solution content. The additional EDX analysis (supporting information S2 available at stacks.iop.org/Nano/22/065605/mmedia) showed that the compositions of AuPt (1/4) and AuPt

(4/1) were 20.30 to 79.70 and 85.25 to 14.75, which also were reasonably close to the precursor ratios of Au and Pt ions.

Figures 3(a) and (c) are TEM images of the NPs from a solution with 1:1 Au/Pt ratio without and with PEG. The corresponding selected area electron diffraction (SAED) results are shown in figures 3(b) and (d). Without PEG, we see in figure 3(b) the superposition of the fcc ring patterns of Pt and Au NPs. The corresponding TEM micrograph in figure 3(c) reveals small, spherical Au NPs and larger, polyhedral Pt NPs. With PEG, figure 3(d) shows a SAED pattern with rings corresponding to the (111), (200), (311), and (220) planes of fcc AuPt alloy. We evaluated the average NP size from figures 3(c) and (d), obtaining 2.36 nm for the alloyed NPs, compared with 4.86 and 2.72 nm for PEG–Au NPs and PEG–Pt NPs revealed in figure 4. The smaller size of the alloyed NPs can be attributed to the initial nucleation process [18].

Figure 5(a) shows a high-resolution TEM (HRTEM) micrograph of a single AuPt NP, revealing the [011] lattice of the AuPt alloy. The corresponding FFT (fast Fourier transform) pattern of figure 5(b) clearly shows the single crystal structure.

The FTIR measurements as shown in figure 6 revealed the existence of PEG molecules on the alloyed AuPt NP surface. Vibrational bands due to PEG were indeed detected, including the $CH_2$ group (2850–2950 cm$^{-1}$) and the C–O–C stretching band (1000–1200 cm$^{-1}$). A broad band at 3200–3600 cm$^{-1}$ related to the hydroxyl (OH) group could be due to hydrogen bond formation between the NP surface and PEG.

The specific mechanisms underlying the production of alloyed NP with synchrotron x-ray irradiation in the presence
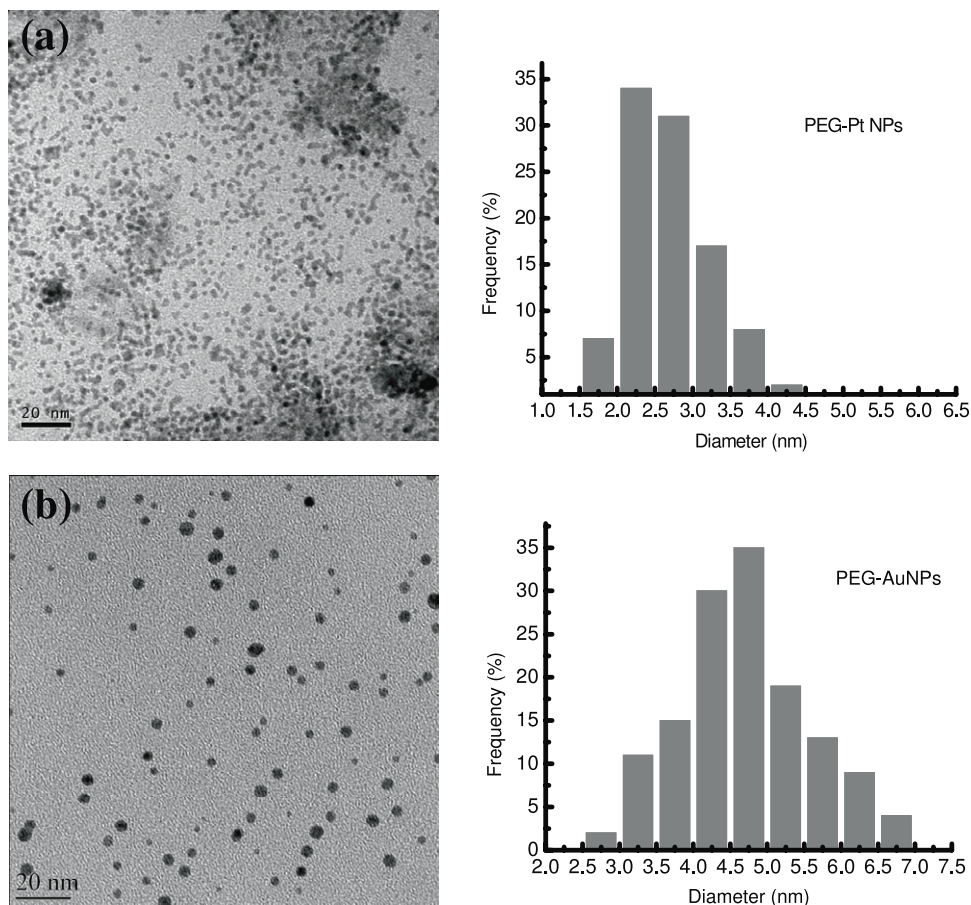
**Figure 4.** TEM images of (a) PEG–Pt NPs and (b) PEG–Au NPs, and their corresponding size distribution diagrams.
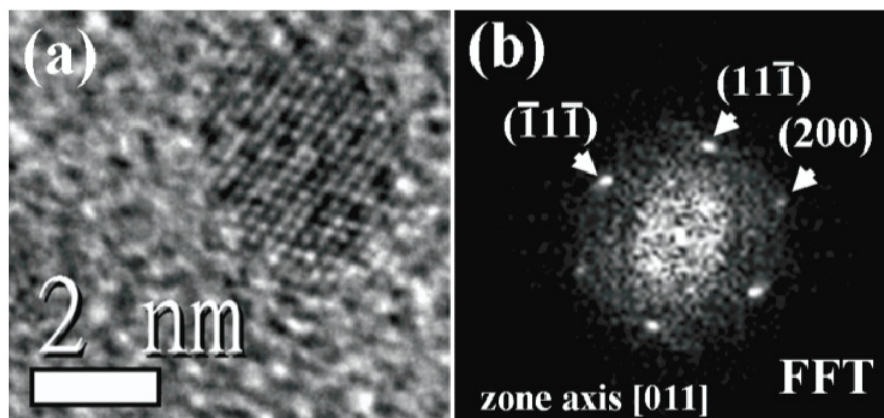


**Figure 5.** HRTEM image of a single alloyed NP synthesized from a solution with 1:1 Au/Pt ratio with PEG, and its corresponding FFT pattern along the [011] direction.

of PEG must still be entirely clarified. We can propose the following arguments. With a slow reduction process, the element with the faster reduction would start nucleating as monometallic NPs before the other is sufficiently reduced. The high intensity of synchrotron light makes it possible instead to reduce both elements in a very short time, minimizing this effect.

However, fast reduction is not sufficient to obtain alloyed NPs. If the growth of an alloyed particle continues beyond the initial nucleation stage, for example by coalescence with other alloyed NPs, phase segregation is likely to take place. Since no metallic Au or Pt was seen by UV–vis spectroscopy and XRD after irradiation with PEG, segregation can be ruled out. This can be explained by assuming that PEG stops the growth of alloyed NPs after the initial nucleation.

The combined effects of PEG and irradiation yield alloyed AuPt NP colloids with high stability and, as seen in figure 3(c), a narrow NP size distribution. This
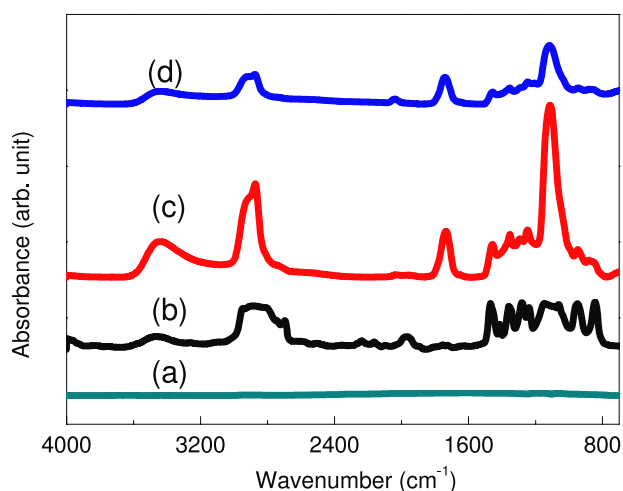
**Figure 6.** FTIR spectra of AuPt NPs without PEG (a), PEG (b), PEG–Pt NPs (c), and PEG–AuPt NPs (d).

confirms the positive impact of PEG on the irradiation-stimulated NP synthesis, previously observed for Ag [34], Au [37] and other systems. Furthermore, cytotoxicity tests (supporting information available at stacks.iop.org/Nano/22/065605/mmedia) indicated a high biocompatibility of our alloyed NPs. We note that the PEG-assisted process described here is chemically clean and involves a small number of ingredients, which are positive aspects for possible applications.

Note, however, that the use of PEG could negatively impact applications that are sensitive to the surface conditions, such as catalysis. However, the PEG can be easily removed, for example by low-temperature annealing. Preliminary tests indicate that such a thermal process would not affect the alloy structure.

## 4. Conclusions

We demonstrate with a successful test that AuPt alloyed nanoparticles with variable composition in colloidal solution can be synthesized with small size and quite uniform size distribution by a one-pot procedure based on synchrotron x-ray irradiation in the presence of PEG (polyethylene glycol). The alloyed nanoparticles are found to be of fcc structure and the composition of the AuPt alloyed nanoparticles can be varied in a continuous fashion by simply varying the feed ratios of Au and Pt precursors. This is possible due to the extremely fast reduction of precursors by the very intense x-rays without relying on any additional chemical reduction agent. We also find that these nanoparticles exhibit high colloidal stability and biocompatibility, quite important for potential applications, possibly due to the relatively simple chemistry.

## References

[1] Thomas J M, Raja R, Johnson B F G, Hermans S, Jones M D and Khimyak T 2003 *Ind. Eng. Chem. Res.* **42** 1563–70
[2] Bronstein L M, Chernyshov D M, Volkov I O, Ezernitskaya M G, Valetsky P M, Matveeva V G and Sulman E M 2000 *J. Catal.* **196** 302–14
[3] Chushak Y G and Bartell L S 2003 *J. Phys. Chem.* B **107** 3747–51
[4] Lu L, Sun G, Zhang H, Wang H, Xi S, Hu J, Tian Z and Chen R 2004 *J. Mater. Chem.* **14** 1005–9
[5] Hultgren R, Desai P D, Hawkins D T, Gleiser M and Kelley K K 1973 *Selected Values of the Thermodynamic Properties of Binary Alloys* (Metals Park, OH: American Society for Metal)
[6] Massalski T B, Murry J L, Bennett L H and Baker H 1986 *Binary Alloy Phase Diagram* vol 1 (Metals Park, OH: American Society for Metal)
[7] Kim S J and Jang D 2008 *J. Mater. Lett.* **62** 4500–2
[8] Rossi G, Rapallo A, Mottet C, Fortunelli A, Baletto F and Ferrando R 2004 *Phys. Rev. Lett.* **93** 105503
[9] Darby S, Jones T V, Johnston R L and Roberts C 2002 *J. Chem. Phys.* **116** 1536–50
[10] Aguado A, Gonzalez L E and Lopez J M 2004 *J. Phys. Chem.* B **103** 11722–31
[11] Mott D, Luo J, Njoki P N, Lin Y, Wang L and Zhong C 2007 *J. Catal. Today* **122** 378–85
[12] Lou Y, Maye M M, Han L, Luo J and Zhong C 2001 *J. Chem. Commun.* **5** 473–4
[13] Stamenkovic V R, Mun B S, Arenz M, Mayrhofer K J J, Lucas C A, Wang G, Ross P N and Markovic N M 2007 *Nat. Mater.* **6** 241–7
[14] Fukuoka A, Higashimoto N, Sakamoto Y, Inagaki S, Fukushima Y and Ichikawa M 2002 *Top. Catal.* **18** 73–8
[15] Mariscal M M, Dassie S A and Leiva E P M 2005 *J. Chem. Phys.* **123** 184505
[16] Xiao S, Hu W, Luo W, Wu Y, Li X and Deng H 2006 *Eur. Phys. J.* B **54** 479–84
[17] Wu M L, Chen D H and Hung T C 2001 *Chem. Mater.* **13** 599–606
[18] Liz-Marzán L M and Philipse A P 1995 *J. Phys. Chem.* **99** 15120–8
[19] Wang C H, Liu C J, Wang C L, Chien C C, Hwu Y, Liu R S, Yang C S, Je J H, Lin H M and Margaritondo G 2009 *Appl. Phys. A* **97** 295–300
[20] Sachdev A and Schwank J 1989 *J. Catal.* **120** 353–69
[21] Shen J, Hill J M, Ramachandra M W, Podkolzin S G and Dumesic J A 1999 *Catal. Lett.* **60** 1–9
[22] Mihut C, Descorme C, Duprez D and Amiridis M D 2002 *J. Catal.* **212** 125–35
[23] Njoki P N, Luo J, Wang L, Maye M M, Quaizar H and Zhong C J 2005 *Langmuir* **21** 1623–8
[24] Luo J, Njoki P N, Mott D, Wang L and Zhong C J 2006 *Langmuir* **22** 2892–8
[25] Damle C, Biswas K and Sastry M 2001 *Langmuir* **17** 7156–9
[26] Zhou S, Jackson G S and Eichhorn B 2007 *Adv. Funct. Mater.* **17** 3099–104
[27] Xu J, Zhao T, Liang Z and Zhu L 2008 *Chem. Mater.* **20** 1688–90
[28] Nakanishi M, Takatani H, Kobayashi Y, Hori F, Taniguchia R, Iwasea A and Oshima R 2005 *Appl. Surf. Sci.* **241** 209–12
[29] Rosenberg R A, Ma Q, Lai B and Mancini D C 1998 *J. Vac. Sci. Technol.* B **16** 3535–8

[30] Ma Q, Moldovan N, Mancini D C and Rosenberg R A 2000 *Appl. Phys. Lett.* **76** 2014–6

[31] Yang Y C, Wang C-H, Hwu Y and Je J H 2006 *Mater. Chem. Phys.* **100** 72–6

[32] Wang C H *et al* 2007 *Mater. Chem. Phys.* **106** 323–9

[33] Wang C H, Chien C C, Yu Y L, Liu C J, Lee C F, Chen C H, Hwu Y, Yang C S, Je J H and Margaritondo G 2007 *J. Synchrotron Radiat.* **14** 477–82

[34] Borse P H, Yi J M, Je J H, Choi S D, Hwu Y, Ruterana P and Nouet G 2004 *Nanotechnology* **15** S389–92

[35] Doudna C M, Bertino M F, Blum F D, Tokuhiro A T, Lahiri-Dey D, Chattopadhyay S and Terry J 2003 *J. Phys. Chem.* B **107** 2966–70

[36] Karadas F, Ertas G, Ozkaraoglu E and Suzer S 2005 *Langmuir* **21** 437–42

[37] Wang C H *et al* 2008 *J. Phys. D: Appl. Phys.* **41** 195301